

Interaction between cognitive and motor cortico-basal ganglia loops during decision making: a computational study

M. Guthrie, A. Leblois, A. Garenne and T. Boraud

J Neurophysiol 109:3025-3040, 2013. First published 27 March 2013;
doi: 10.1152/jn.00026.2013

You might find this additional info useful...

This article cites 86 articles, 32 of which you can access for free at:
<http://jn.physiology.org/content/109/12/3025.full#ref-list-1>

Updated information and services including high resolution figures, can be found at:
<http://jn.physiology.org/content/109/12/3025.full>

Additional material and information about *Journal of Neurophysiology* can be found at:
<http://www.the-aps.org/publications/jn>

This information is current as of June 17, 2013.

Interaction between cognitive and motor cortico-basal ganglia loops during decision making: a computational study

M. Guthrie,^{1,2} A. Leblois,^{3,4} A. Garenne,^{1,2} and T. Boraud^{1,2}

¹Institut des Maladies Neurodégénératives, Université Bordeaux-Segalen, UMR 5293, Bordeaux, France; ²Institut des Maladies Neurodégénératives, Centre National de la Recherche Scientifique, UMR 5293, Bordeaux, France; ³Laboratoire de Neurophysique et Physiologie, Université Paris Descartes, UMR 8119, Paris, France; ⁴Laboratoire de Neurophysique et Physiologie, Centre National de la Recherche Scientifique, UMR 8119, Paris, France

Submitted 11 January 2013; accepted in final form 23 March 2013

Guthrie M, Leblois A, Garenne A, Boraud T. Interaction between cognitive and motor cortico-basal ganglia loops during decision making: a computational study. *J Neurophysiol* 109: 3025–3040, 2013. First published March 27, 2013; doi:10.1152/jn.00026.2013.—In a previous modeling study, Leblois et al. (2006) demonstrated an action selection mechanism in cortico-basal ganglia loops based on competition between the positive feedback, direct pathway through the striatum and the negative feedback, hyperdirect pathway through the subthalamic nucleus. The present study investigates how multiple level action selection could be performed by the basal ganglia. To do this, the model is extended in a manner consistent with known anatomy and electrophysiology in three main areas. First, two-level decision making has been incorporated, with a cognitive level selecting based on cue shape and a motor level selecting based on cue position. We show that the decision made at the cognitive level can be used to bias the decision at the motor level. We then demonstrate that, for accurate transmission of information between decision-making levels, low excitability of striatal projection neurons is necessary, a generally observed electrophysiological finding. Second, instead of providing a biasing signal between cue choices as an external input to the network, we show that the action selection process can be driven by reasonable levels of noise. Finally, we incorporate dopamine modulated learning at corticostriatal synapses. As learning progresses, the action selection becomes based on learned visual cue values and is not interfered with by the noise that was necessary before learning.

action selection; cortico-basal ganglia loops; computational models; dopamine; learning

DECISION MAKING IS A HIGH-level brain function under the control of a distributed network of cortical and subcortical structures, interconnected in positive and negative feedback loops determined by the anatomical connectivity and polarity of the basal ganglia nuclei (Mink 1996; Redgrave et al. 1999). Box and arrow models of basal ganglia connectivity demonstrate the polarity of these anatomical pathways (Albin et al. 1989; Alexander et al. 1991), but cannot show how selection between two possible actions is performed by the network. Mink (1996) proposed a schematic basal ganglia action selection model based on this anatomy. Using this center-surround architecture, he postulated that separate cortical networks are activated for each of a set of possible actions. The divergent, negative feedback hyperdirect pathway first provides widespread and rapid cortical inhibition to hold the release of all proposed actions. The positive feedback direct pathway then gives a

more localized disinhibition that amplifies any difference in activation between the competing cortical networks to select one specific action.

Beyond the box and arrow model, it has also been proposed that there are several parallel, segregated, direct pathway loops through the basal ganglia connecting back to distinct areas of cortex, each involved in a different modality of action selection (Alexander et al. 1986). However, there are complexities of convergence and divergence within the pathways that suggest that the parallel loops cannot be completely segregated (See MATERIALS AND METHODS, *Model architecture*).

Recent electrophysiological data from Pasquereau et al. (2007), in primates, suggest that, in a two-armed bandit task, two separable processes occur during action selection. First, early changes in globus pallidus (GPI) activity, when the two cue shapes are presented, are related to the cognitive aspect of the task and express the decision of which of the cue shapes has a greater value. Then, when a subsequent signal to move is given, changes in GPI activity are related to the motor aspect of the task and reflect the preparation of the motor action necessary to express the selection of the chosen cue. Thus, in this task, the full action selection process is separable into two, temporally distinct, selections each at a different level.

Based on this analysis, we present a biophysically based, two-level model of action selection that can solve the task used in Pasquereau et al. (2007), using the minimum details of brain circuitry necessary. The model comprises two action selection modules: one for solving the cognitive action selection, and the other for solving the motor action selection. Each module consists of one instance of the center-surround architecture of Mink (1996), and the two modules are considered to be parallel, with inputs from distinct areas of cortex. In the model, when discussing the separation of action selection into two levels, we define a level as being a loop in which an area of cortex is in closed-loop feedback through the basal ganglia with itself (a cortico-basal ganglia or CBG loop) and channels as separate ensembles within that cortical area, each representing a possible decision choice, that are in competition with one another during action selection.

The model instantiation is based on that of Leblois et al. (2006) that showed selection between two channels in one CBG loop. The module of action selection consists of a segregated, positive feedback direct pathway and a negative feedback hyperdirect pathway that is widely divergent from the subthalamic nucleus (STN) to GPI. Action selection is an

Address for reprint requests and other correspondence: M. Guthrie, Institut des Maladies Neurodégénératives, UMR CNRS 5293, 146, rue Leo Saignat, 33 076 Bordeaux Cedex, France (e-mail: martin.guthrie@u-bordeaux2.fr).

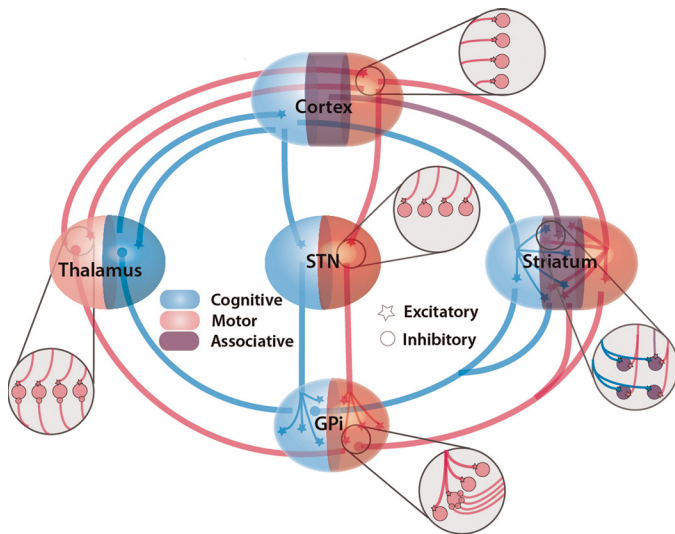


Fig. 1. Architecture of the basal ganglia model. Two cortico-basal ganglia loops are modeled, representing two levels of decision making: a cognitive loop in blue, and a motor loop in red. Each loop consists of a focused, positive feedback, direct pathway loop [cortex-striatum-globus pallidus (GPi)-thalamus-cortex] and a divergent, negative feedback, hyperdirect pathway loop [cortex-subthalamic nucleus (STN)-GPi-thalamus-cortex]. Action selection within each loop is an emergent property of the interaction of the direct and hyperdirect pathways. Information flow from one loop to another is via divergence and reconvergence of the direct pathway. Each direct pathway loop diverges from cortex to associative areas of striatum. The associative striatum then has outputs to both motor and cognitive GPi. The action selection made in the cognitive corticostriatal loop is passed to the motor corticostriatal loop via this divergence and convergence and is used to bias the motor decision. Within each loop, separate channels represent the decision choices at that level. Competition for expression occurs between these channels at that level. Association cortex projects to associative striatum (purple), but is not involved in a closed feedback loop. Expansions of inputs to each structure are shown in circles. To avoid confusion, only the inputs are shown; the outputs can be deduced from the main diagram. The expansions of cortex and STN show simple 1:1 excitatory inputs. The expansion of the striatum shows 2 cognitive corticostriatal neurons (in blue), each diverging to innervate 2 associative striatal neurons, 2 motor corticostriatal neurons (in red) diverging to innervate a different set of associative striatal neurons, and an associative corticostriatal neuron (in purple) innervating a single associative striatal neuron. Inputs from cognitive (motor) cortex to cognitive (motor) striatum are topographic. The expansion of the GPi shows a divergent STN neuron innervating all 4 GPi neurons and 4 associative striatal neurons converging to innervate a single GPi neuron. As with the corticostriatal connection, inputs from cognitive (motor) striatum to cognitive (motor) GPi are topographic. The expansion of the thalamus shows the topographic inhibitory inputs from the GPi and the topographic excitatory feedback from the cortex that forms a corticothalamic positive feedback loop.

intrinsic property of the interaction between the direct and hyperdirect pathways.

In the Leblois et al. (2006) model, a biasing signal was applied to one channel to cause symmetry breaking between channels and thus selection of one action. Here, the symmetry breaking is caused by introduced synaptic noise. Each CBG loop comprises an identical action selection module. To solve the task correctly, the decision made at the cognitive level must be available to guide the decision at the motor level. The information transfer between the two levels occurs at the level of the striatum (Fig. 1). The model also incorporates learning, modulated by a simulated dopamine reward signal to form a type of actor-critic network (Barto 1995). The learning is used to demonstrate that changes in relative gain between two channels in one corticostriatal loop are sufficient to derive

robust action selection, taking over from the noise as the driver of symmetry breaking. In contrast to previous actor-critic models (Brown et al. 1999; Suri and Schultz 1999), we chose to model the critic at a very basic level, to concentrate on the mechanisms underlying action selection in the actor. We show that this architecture only works to perform accurate two-level decision making when the striatal neurons are difficult to excite, one of the basic observed properties of striatal projection neurons (Wilson and Groves 1981).

MATERIALS AND METHODS

Task. This center-out motor task has been fully described in Pasquereau et al. (2007), where electrophysiological data were obtained during the performance of the task by macaque monkeys. During a simulation, consisting of 120 trials, four cues were used, each with a different reward probability $\{P(R) \in [0, 0.33, 0.66, 1]\}$ (Fig. 2). For each trial, two of the cues were presented. After the decision is made of which direction to move, the reward probability of the chosen target is used to determine if a reward is given or not.

Model architecture. The module of action selection consists of an interacting hyperdirect and direct pathway in one CBG loop, within which there are multiple channels. At a given decision-making level, competition is between the channels of one loop (Fig. 3). Each possible cue shape and motor movement direction is represented by one cortical ensemble. On a given trial with two cue shapes presented at two positions, only two cognitive, two motor, and two association cortex ensembles are activated.

To implement two-level action selection, the current model exploits the separation of the basal ganglia into multiple parallel loops (Alexander et al. 1991). The two loops modeled each represent a level of decision making and consist of two action selection modules in parallel: one for making the selection between two presented cue shapes, and the other for making the selection between two possible movement directions. The selection of shape is assumed to belong to the cognitive domain, i.e., to occur in a more frontal segregated loop than the selection of direction. The actual source of the inputs would probably best be described as visual and visuo-spatial, respectively. Because these two terms are very similar, we persist with the use of cognitive and motor to differentiate the two loops in this paper. However, these terms are used mostly for ease of description, as the architecture would work with any two partially segregated CBG

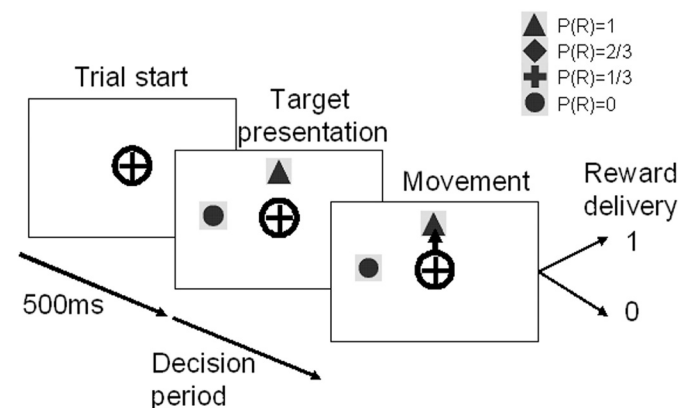


Fig. 2. Center-out action selection task. During a session of 120 trials, 4 cues with different probabilities of reward $[P(R)]$ are used. At each trial, 2 of the 4 cues are pseudorandomly chosen (such that each of the 6 possible pairs is seen 20 times during a session) and presented in randomly chosen cardinal positions. Each trial starts with a period of 500 ms to allow the network to settle, after which the 2 cues are presented. The model selects a direction to move in during the decision period. After selecting a movement, the model receives reward based on the reward probability of the cue shape associated with the direction chosen.

loops, no matter the physical brain location of the originating cortical inputs.

To be meaningful, it is necessary that the decision at one level influence the decision at the other level. There would be no point in selecting a cue shape based on likelihood of reward for that shape and then selecting a movement toward the other shape. The model uses evidence that the loops cannot be entirely separate to suggest an architecture where there is divergence in the corticostriatal connection and then reconvergence within the GPi (Graybiel et al. 1994; Parent et al. 2000). Pyramidal cortical neurons have a somatotopic projection to striatum (Webster 1961), but also arborize within the striatum (Cowan and Wilson 1994; Wilson 1987; Parent et al. 2000; Parthasarathy et al. 1992), usually with specific localized areas of bouton formation (Kincaid et al. 1998), and specific small cortical areas innervate the striatum in a discontinuous pattern with areas of denser innervation separated by areas of sparse innervation (Brown et al. 1998; Flaherty and Graybiel 1991). There is also a large reduction in the number of neurons from cortex to striatum to GPi (Bar Gad and Bergman 2001; Oorschot 1996). These findings combined lead to striatal areas that are mostly specific for input from one cortical area alongside areas where there is overlap between inputs from two or more cortical areas (Takada et al. 2001) and which are here referred to as associative striatum.

This pattern of innervation is modeled as a somatotopic input from cognitive cortex to cognitive striatum, and then divergence to specific adjacent areas of associative striatum, and, similarly, from motor cortex to motor striatum and adjacent areas of associative striatum. There is thought to be some convergence from striatum to GPi because the disklike arrangement of GPi dendrites perpendicular to incoming striatal axons would maximize the potential convergence of striatal neurons (Percheron et al. 1984). Also nearby sites in putamen have been shown to have little overlap in GPi projection (Hazrati and Parent 1992c), and injection of a retrograde tracer into GPi leads to labeling of several distinct areas in striatum (Flaherty and Graybiel 1993; Graybiel et al. 1994). This is modeled as a reconvergence from the arborizations of the corticostriatal connection back to somatotopic areas of GPi.

With this divergence and reconvergence of the direct pathway within one loop, one cognitive (motor) cortical channel is involved in a closed positive feedback CBG loop only with its own cognitive (motor) channel within its own cognitive (motor) loop (Fig. 3, A and C). However, the divergence from cortex to association striatum, followed by the two-way reconvergence of associative striatal areas to both cognitive and motor GPi, provides cross talk from one loop to the other (Fig. 3E). This cross talk is, in theory, bidirectional but is only exploited in one direction in the current model because only the shapes have different values, not the directions.

The hyperdirect pathway projects somatotopically from cognitive (motor) cortex to STN (Nambu et al. 1996) and thence diverges widely to cognitive (motor) GPi (Hazrati and Parent 1992a, 1992b). With the somatotopic return of the output of GPi to cortex, one cognitive (motor) cortical channel thus provides negative feedback to all cognitive (motor) cortical channels via the hyperdirect pathway of that loop (Fig. 3, B and D).

Association cortex inputs to the striatum are assumed to be a high-level visual representation that is a conflation of both the cue shape and position. This is taken as arising from parietal cortical areas. These more dorsal cortical inputs do not form closed loops with the basal ganglia and are only an input to associative striatum (Fig. 3F).

Neuronal dynamics. As in the Leblois et al. (2006) study, a neuronal rate model is used (Hopfield 1984; Shriki et al. 2003; Wilson and Cowan 1972) to keep neuronal dynamics simple and focus on the network dynamics. Each set of coactivated neurons, an ensemble, within each structure is modeled as a single rate neuron with the following equation:

$$\tau \frac{dm}{dt} = -m + I_s + I_{\text{Ext}} - T \quad (1)$$

where τ is the decay time constant of synaptic input, m is the output of the neuron, I_s is the synaptic input to the ensemble, I_{Ext} is an external input representing the sensory visual salience of the cue, and T is the threshold of the neuron. Negative values of activation, m , were set to zero. Temporal integration of output was performed using a standard first-order Euler algorithm with 1-ms step. The parameters for τ and T for each structure are shown in Table 1. A negative threshold means that, at steady state, with no input, the neuron has an output equal to that threshold. At each time step Gaussian distributed noise is added to the synaptic input of each ensemble with the mean being a percentage of the external synaptic input, as shown in Table 1.

The gain of the synaptic connection from *population A* (presynaptic) to *population B* (postsynaptic) is denoted as G_B^A , and the total synaptic input to *population B* is:

$$I_s^B = \sum_A G_B^A m_A \quad (2)$$

where A is the presynaptic ensemble, B is the postsynaptic ensemble, and m_A is the output of presynaptic ensemble A . The gains for each pathway are shown in Table 2. Gains to the corresponding cognitive (motor) ensemble are initially five times higher than to each receiving associational area. Reconvergence from cognitive (motor) and association areas of striatum to cognitive (motor) areas of GPi are evenly weighted.

Striatal transfer function. Striatal projection neurons are generally silent at rest (Sandstrom and Rebec 2003), require concerted coordinated input to cause firing (Wilson and Groves 1981), and have a sigmoidal *IV* function (nonlinear relationship between input current and membrane potential) due to both inward and outward potassium current rectification (Nisenbaum and Wilson 1995). This is modeled by applying a sigmoidal transfer function to the activation of corticostriatal inputs in the form of the Boltzmann equation:

$$m_{\text{out}} = V_{\text{min}} \cdot \left(\frac{V_{\text{max}} - V_{\text{min}}}{1 + e^{-\frac{V_h - m_{\text{in}}}{V_c}}} \right) \quad (3)$$

where m_{in} is the input to the transfer function (the activation level of the cortical inputs in this case) and m_{out} is the output, V_{min} is the minimum activation, V_{max} the maximum activation, V_h the half-activation, and V_c the slope. This is similar to the use of the output threshold in the Gurney (Gurney et al. 2001) model and results in small or no activation to weak inputs with a rapid rise in activation to a plateau level for stronger inputs. The parameters used for this transfer function are shown in Table 3 and were selected to give a low striatal output with no cortical activation [1 spikes (sp)/s], starting to rise with a cortical input of 10 sp/s and a striatal output of 20 sp/s at a cortical activation of 30 sp/s (see Fig. 8A, *inset* shows the curve produced).

Decision making. For each trial, two out of a set of four cues were shown, each in a randomly chosen cardinal position (North, East, South, West; excluding cue superposition).

Before the cues were presented, the model was run for 500 ms to allow the system to settle into its fixed point. When the cues were shown, the two cognitive cortical ensembles representing the shapes of the shown cues, the two motor cortical ensembles representing the directions to move to reach the two cues, and the two associative cortical ensembles representing a conflation of cue shape and direction received an additional external input, I_{Ext} (Eq. 1), representing the visual salience of the cue shape and direction. This salience is an intrinsic property of the visual stimulation of the cue (Itti and Koch 2001), does not change with learning, and was preset at 7 sp/s. A negative threshold of 3 sp/s was used for cortical neurons to simulate a low at-rest firing rate (Table 1), giving a total activation of 10 sp/s when the cues were present.

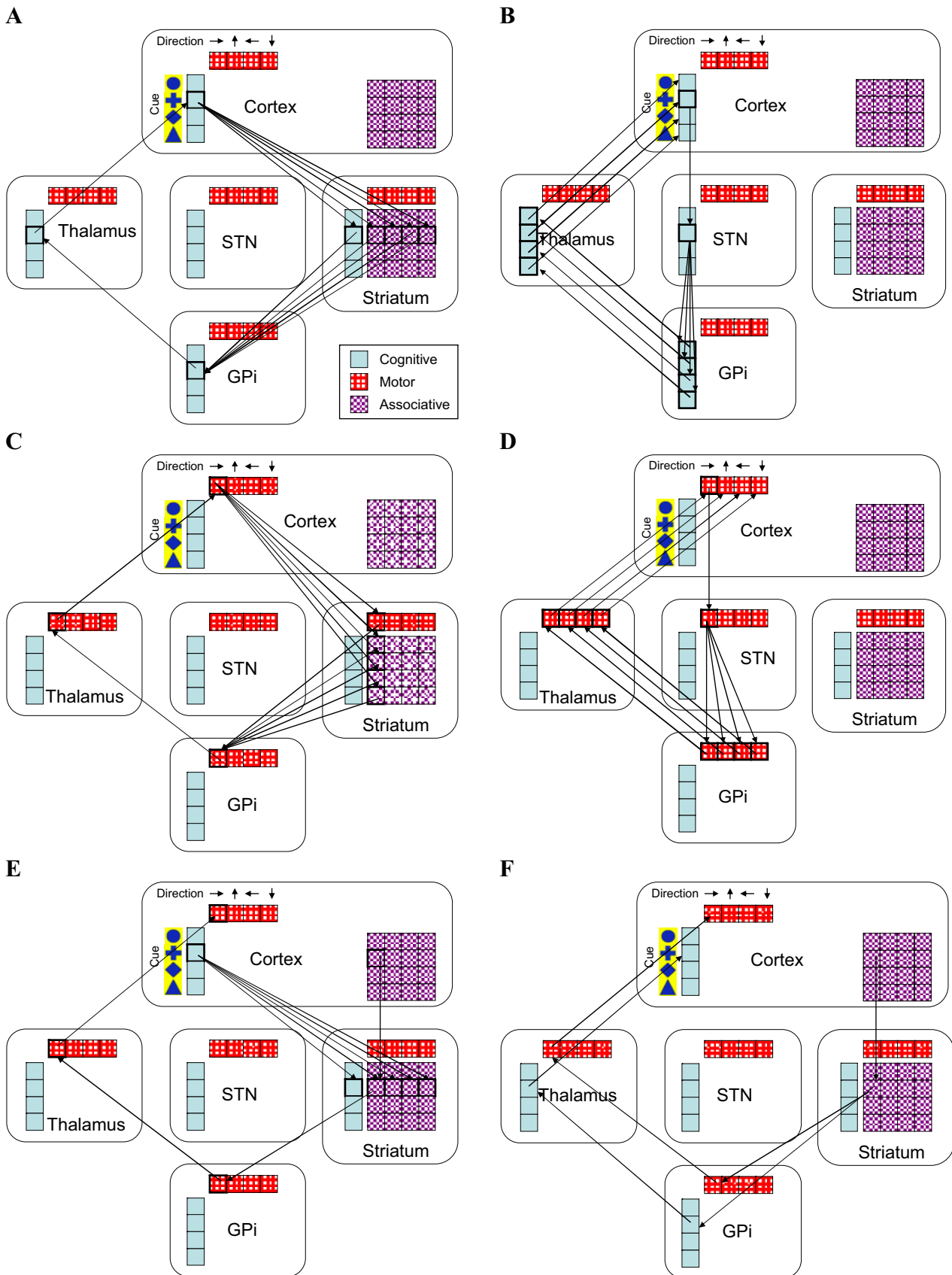


Table 1. Model neuron parameters in each network structure

	Synaptic Decay (τ)	Threshold (T)	Noise, %
Cortex	10	-3	1
Striatum	10	0	1
STN	10	-10	1
GPI	10	10	3
Thalamus	10	-40	1

STN, subthalamic nucleus; GPI, globus pallidus.

A movement was deemed to have occurred when the activation of one motor cortical ensemble was 40 sp/s greater than that of any other. A trial was considered successful if a movement occurred in less than 2.5 s after the cues were presented and optimum if the movement was toward the shape with the higher reward probability.

Learning. In learning simulations, each run consisted of 120 trials so that each context (combination of 2 out of the 4 cues, 6 possible combinations) was presented 20 times. The learning rules were applied after each trial.

In the model, learning occurs only at the corticostriatal synapse where phasic changes in dopamine concentration have been shown to be necessary for the production of long-term potentiation (LTP) (Kerr and Wickens 2001; Pawlak and Kerr 2008; Reynolds et al. 2001). There may be learning in other structures and pathways within the basal ganglia, but the aim here was to show that corticostriatal direct pathway learning was sufficient of itself to produce the behavior under consideration.

The corticostriatal weight is used as a multiplier to the corticostriatal pathway gain to keep the factors of gain and weight separately observable, although in reality both would be represented together in the corticostriatal synapse. The synaptic current from cortical *ensemble A* to striatal *ensemble B* is given by:

$$I_S^B = \sum_A w_B^A \cdot G_B^A \cdot m_A \quad (4)$$

where w_B^A is the weight of the connection from cortical *ensemble A* to striatal *ensemble B*. At the start of each run, all synaptic weights were initialized to 0.5 (SD 0.005). After each trial, the corticostriatal weights are updated.

$$\Delta w_B^A = PE \cdot \alpha_a \cdot m_B \quad (5)$$

where Δw_B^A is the change in the weight of the corticostriatal synapse from cortical *ensemble A* to striatal *ensemble B*, PE is the prediction error, the amount by which the actual reward delivered differs from the expected reward, m_B is the activation of the striatal ensemble, and α_a is the global actor learning rate. Generation of LTP and long-term depression (LTD) in striatal MSNs has been found to be asymmetric (Pawlak and Kerr 2008). Therefore, in the model, the actor learning rate is different for LTP and LTD. For LTP, α_a is 0.002; for LTD, 0.001. The PE is calculated using a simple critic learning algorithm.

$$PE = R - V_i \quad (6)$$

where R, the reward, is 0 or 1, depending on whether a reward was given or not on that trial. Whether a reward was given was based on the reward probability of the cue associated with the direction chosen.

Table 2. Standard gains of all pathways in the network

From Population A	To Population B	Pathway	Gain (G)
Cortex	Striatum	cognitive → cognitive	1
		motor → motor	1
		associative → associative	1
		cognitive → associative	0.2
Striatum	STN	motor → associative	0.2
		cognitive → cognitive	1
		motor → motor	1
		associative → both	2
STN	GPI	cognitive → cognitive	1
		motor → motor	1
GPI	Thalamus	cognitive → cognitive	0.5
		motor → motor	0.5
Thalamus	Cortex	cognitive → cognitive	1
		motor → motor	1
Cortex	Thalamus	cognitive → cognitive	1
		motor → motor	1

i is the number of the cue chosen, and V_i is the value of cue i . The value of the chosen cue is then updated using the PE.

$$V_i \leftarrow V_i + (PE \cdot \alpha_c) \quad (7)$$

where α_c is the critic learning rate, set to 0.05.

Corticostriatal weights are bounded by a sigmoidal transfer function (Table 4) to represent physical constraints on synaptic growth with an absolute maximum of 0.75 and an absolute minimum of 0.25. These limits are conservative and were selected to show that action selection can be learned with very small changes in synaptic weights in this model.

Tools. The model was written in Delphi 7 (Borland 2001). All data, including model setup information, were automatically saved to Excel (Microsoft, 2003) after each trial of a simulation and automatically summarized at the end of each simulation. Regression coefficients were calculated in Matlab using custom software.

Comparison with experimental data. We also analyzed how neurons from these populations could be classified using statistical methods previously used in electrophysiology. From a series of 10 runs of 180 trials, the last 140 trials were selected to rule out the learning period. For these trials, the correlation between the modulation of firing rate of the ensembles was analyzed using a three-way ANOVA (Selected Shape × Unselected Shape × Direction, $P < 0.05$), followed by a Fisher post hoc, test on the value of m when it reached the selection level. We therefore classified neurons as responding to Direction (A for Action), Selected Shape (Cv for Chosen value), Unselected Shape (NCv for Non-Chosen value), Direction and Selected Shape (Av for Action value), and Both Shapes (St for State). We applied the same method to the experimental data previously published (Woodward et al. 1995). The value used for the neuronal response was extracted from a Peri-Stimulus Time Histogram centered on movement onset with 20-ms bins and smoothed with a Gaussian window, $\sigma = 60$ ms. The average firing rate was normalized

Fig. 3. Architecture of action selection model. *A*: the direct pathway from cognitive cortical ensembles is divergent from cortex to cognitive striatum and one row of associative striatum. The striatal row then reconverges in one cognitive GPI area and thus forms a closed loop with the original cognitive cortical ensemble. *B*: the hyperdirect pathway from cognitive cortical ensembles is widely divergent from STN to GPI, innervating all cognitive, but not motor, GPI regions and thus feeds back to all cognitive cortical ensembles. *C*: the motor direct pathway is divergent to cognitive striatum and one column of associative striatum and reconverges on motor GPI as for the cognitive cortical input. *D*: as for the cognitive hyperdirect pathway, the motor hyperdirect pathway is divergent to all motor areas of GPI. *E*: due to convergence of motor and cognitive pathways in association striatum, the cognitive pathway feeds back not only to the cognitive cortical area that it originated from, but also to motor cognitive areas, allowing the feed-forward of a decision made in cognitive loops to influence the decision in motor loops. In this figure, the feed-forward is shown from only one area of associational striatum to one area of motor cortex, but each area of associational striatum feeds back to the corresponding column of motor cortex. *F*: association cortex ensembles are open loop to both cognitive and motor cortex.

Table 3. Parameters for striatal sigmoidal transfer function

Parameter	Value
V_{\min}	1
V_{\max}	20
V_h	16
V_c	3

V_{\min} , minimum activation; V_{\max} , maximum activation; V_h , half-activation; V_c , slope.

by subtracting base activity recorded during intertrial interval and averaged for 200 ms before to 300 ms after.

RESULTS

Dynamic action selection. We first show that the internal noise is sufficient to bring about the symmetry breaking that is a prerequisite of action selection and will allow the system to explore possible actions. In a single trial before learning, where all corticostriatal weights are set to 0.5 with no variation, action selection in the model is reliant on synaptic noise to generate a bias toward one channel. In simulations with no noise, no action selection occurred (data not shown). The evolution of the activation of the cortical channels is shown in Fig. 4, with the two cognitive channels representing the cue shapes in black and the two motor channels representing the directions in gray. Because there are four possible cue shapes and four possible directions, each loop has four channels. Because only two shapes in two positions are presented on each trial, only two of the four channels are activated on each trial. The remaining two channels remain at the background level of activation.

In the 500 ms before the cues are presented, activations of all channels are similar, varying randomly with synaptic noise. The large negative threshold in thalamus (Table 1) activates the hyperdirect pathway loop, but not the direct pathway, because the striatal transfer function renders the striatal projection neurons insensitive to this level of cortical input.

When the cues are presented ($t = 0$), two cognitive, two motor, and two association cortex ensembles receive external inputs due to the sensory input of the cues. In the following, we will refer to this level of cortical activation as the “salience level” of the external input (due to cue shape in the cognitive loop and cue direction in the motor loop). The salience level does not change with learning and is not related to the cue value learned via reward feedback. Due to the noise in the positive feedback direct pathway, symmetry breaking occurs in each loop after the presentation of the cues as follows. Because the loop gain of the direct pathway is greater than one, differential activation of one channel due to noise is amplified. The resultant increased cortical activation of that channel starts a positive feedback takeoff in that channel, but also increases input to the divergent, negative feedback hyperdirect pathway, causing suppression of all channels, but especially the competing channel. This mechanism is the same as that observed in the Leblois et al. (2006) model, but does not require an additional biasing external input, being due simply to the synaptic noise in the system. Also, the mechanism extends in the present model to two loops in parallel. In the main panel in Fig. 4, the cognitive action selection (black line) occurs before the motor action selection (gray line).

When synaptic weights are the same throughout the network, all cue shapes and directions have the same value. In this

case, the order of the two selection processes is random, and a trial where the motor action selection is made before the cognitive action selection is shown in the *inset*. In this case, the activation of one motor cortical ensemble passes the threshold before any cognitive cortical ensemble has reached this level, so a cognitive decision cannot strictly be said to have been made, but a motor action is still performed.

Based on these simulations, in all subsequent simulations, an action selection threshold of a difference of 40 sp/s between two competing channels was used. As an example, the times for cognitive and motor action selection for the simulation shown in Fig. 4 would be $t = 1,125$ ms and $t = 1,190$ ms, respectively.

Learning of action selection. Each learning simulation consisted of 120 trials. Weights were initialized to a Gaussian distribution with a mean of 0.5 and a SD of 0.005 at the start of each simulation. Figure 5 shows the evolution of choice behavior averaged over 250 simulations. The probability of selecting the optimal cue (the cue with a higher probability of delivering reward) started at chance level (0.5) and increased to 0.95 ± 0.01 during the last 30 trials (Fig. 5, *inset*). The difference between the performance in the first and last 30 trials was highly significant ($P < 0.0001$, one-way ANOVA). Due to the stochastic nature of reward and cue appearance, the level of reward gained remained at $\sim 75\%$ of trials, even at the end of the learning period. The maximum level of reward obtainable with the cue reward probabilities used is 14/18 (77.8%). The learning curve over the 120 trials was fit by an exponential function ($y = 0.5 + 0.5\{1 - \text{Exp}[-(t - 1)/13.7]\}$), where t is the trial number, with $R^2 = 0.95$ (gray curve). See Table 5.

Over the course of the 120 trials, the average corticostriatal weight from cognitive cortex to cognitive striatum evolved under the learning rules to reflect the reward history for each cue. Figure 6 shows that the average weight for the best cue, where reward was certain, increased to 96% of maximum by the end of the run. The weight for the worst cue only decreased to 44% over the course of 120 trials. The standard error bars for the cues where the reward is uncertain [cues with $P(R) = 0.33$, $P(R) = 0.66$] are larger than for the deterministic cues. Figure 6, *inset*, shows the evolution of weights from a single run to illustrate the noisiness of the evolution, particularly for the probabilistic cues.

Figure 7 shows the change in time taken for each level of the action selection. The total time consists of the time taken for the cognitive action selection plus the additional time after this for the motor action selection. On the first trial (Fig. 7A), the time for motor action selection is 0 ms in 54% of cases, indicating that the motor action selection occurred before or at the same time as the cognitive action selection. At the end of learning, on the 120th trial (Fig. 7B), most motor action selections take between 60 ms and 160 ms after the cognitive selection. A proportion still take 0 ms, nearly always in the

Table 4. Parameters for learning sigmoidal transfer function

Parameter	Value
V_{\min}	-0.05
V_{\max}	1
V_h	0.5
V_c	0.1

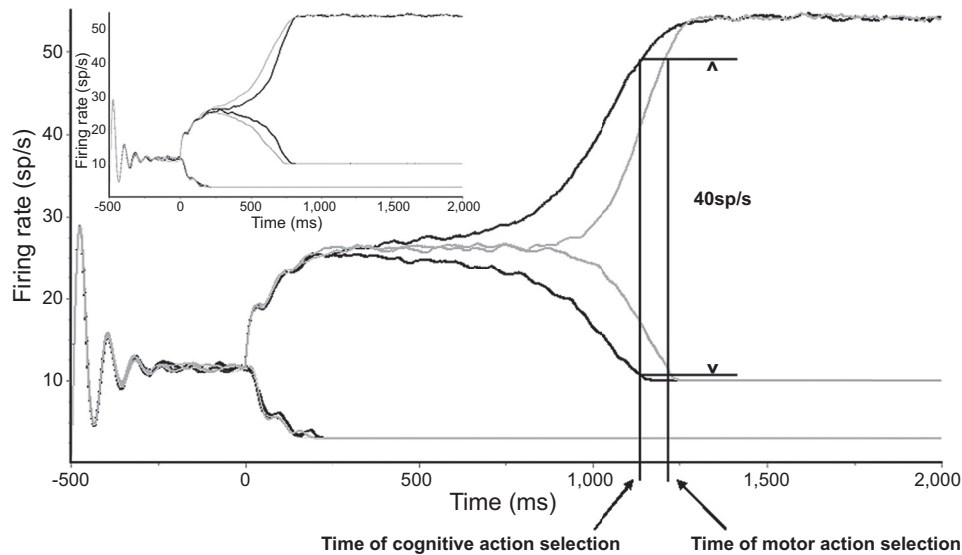


Fig. 4. Activity in the cortical populations during a single trial of action selection. All weights are initialized to 0.5. The network is started at time $t = -500$ ms and allowed to settle to a steady state before the presentation of the cues at $t = 0$. Black lines represent cognitive cortical activations; gray lines motor cortical activations. Before the cues are presented, all cortical ensembles have an activity of 10 spikes (sp)/s, with variation due to synaptic noise in the model (see Table 3). When the two cues are presented, the activity in the cortical ensembles representing the cue shapes and directions that are not shown are suppressed to the background level, 3 sp/s. After 250 ms, the activity in the two cognitive cortical ensembles representing the shape of the two cues shown starts to diverge. The divergence of activity in motor cortical ensembles lags that in cognitive cortex, starting after 800 ms. 1,250 ms after the cues are presented, activity in the populations representing the selected shape and direction reach a plateau. With a selection threshold of 40 sp/s, the cognitive and motor action selections would be made at the times indicated. *Inset*: an example trial during which the motor action selection leads the cognitive action selection.

$P(R) = 0$ v. $P(R) = 0.33$ context (data not shown). This is because learning has caused a decrease in the average weight between cortical and striatal populations coding for the cue shapes (cognitive loop) in this context, so that this average weight is lower than the average corticostriatal weight for the direction (motor loop). Direction is, therefore, chosen more quickly than shape.

Figure 7C shows that the total time for the action selection, the time taken to choose both a shape and a direction, decreased with learning, as does the time for choosing the shape, the cognitive action selection. For clarity in the figure, the time for motor action selection is shown as the duration after the cognitive action selection has been made and is therefore the total – cognitive selection time. When this time for motor action selection is 0 ms, the motor selection occurs either at the same time step or earlier than the cognitive selection. The time for motor action selection increased from 20 to 100 ms in the course of the first 20 trials due to trials in the early stages of

learning where the direction is chosen before the shape (Fig. 7A). Figure 7C, *inset*, shows the decision time for each trial from a single run. Again, this illustrates that, for an individual simulation, the trial-to-trial variation is large.

Interloop information transfer. A consequence of using the transfer of information between loops to bias selection at one level on the basis of selection at another level is that the transfer could bias the wrong channel in the receiving loop. In the case of the current task simulation, this would mean that a cue shape would be selected, but that the direction for the other cue would subsequently be chosen. We define accurate interloop information transfer as when the direction of movement selected in the motor loop is consistent with the cue shape chosen in the cognitive loop, whether or not the better cue shape was chosen. In the first few trials of a run, when weights in both loops were close to equal, the choice of direction was not related to the choice of shape. However, over the course of a complete run of 120 trials, accurate interloop information

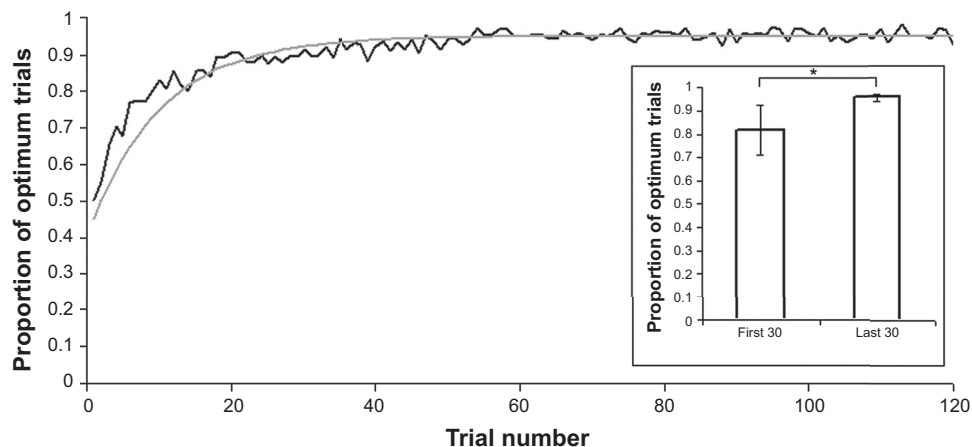


Fig. 5. Learning time course over 120 trials, averaged over 250 simulations. All trials were successful in that a direction was chosen. The learning curve (black) for the choice of the optimum cue could be approximated by an exponential (light gray) $y = 0.5 + 0.5 \times \{1 - \text{Exp}[-(t - 1)/13.7]\}$ with an R^2 of 0.95. Performance reached plateau of ~ 0.95 by the 60th trial. *Inset*: the performance significantly improved in the last 30 trials with respect to the first 30 ($*P < 0.0001$, one-way ANOVA).

Table 5. Parameters for exponential curves to fit learning of each of the six contexts (combination of two cues)

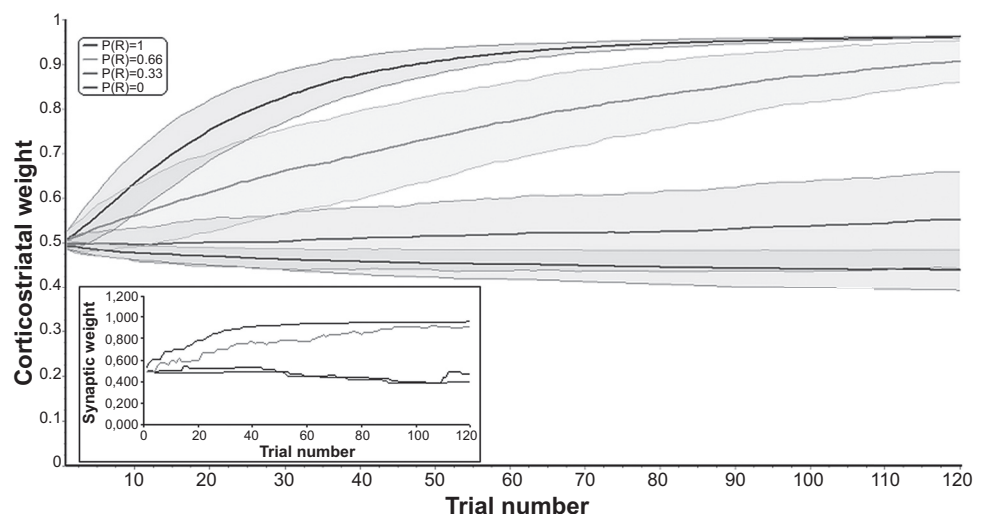
Context	τ	R^2
0 v 0.33	10.9	0.90
0 v 0.66	1.03	0.93
0 v 1	0.35	0.95
0.33 v 0.66	2.82	0.93
0.33 v 1	0.67	0.94
0.66 v 1	3.35	0.88

Each exponential is of the form $y = 0.5 + 0.5\{1 - \text{Exp}[(t - 1)/\tau]\}$, where t is the time step and τ is the time constant for the exponential. R^2 values show how good the fit was for each exponential.

transfer occurred in 99.6% of trials, with each trial being averaged over 250 runs. This performance did not change between the first and last 30 trials, showing that the model learned to choose the direction associated with the chosen cue shape very quickly.

Because the association striatum is the site of convergence and divergence of the two loops, we investigated the correlation between the level of striatal activation with interloop information transfer. The overall striatal activation, which was defined as the count of the 24 striatal ensembles (4 cognitive, 4 motor, 16 associative; Fig. 3) having an activation of >1.5 sp/s at the end of the trial, averaged 4.09 (SD 0.12) over all 120 trials of 250 runs. Simulations were then run with lower values of the striatal transfer function half-activation parameter (V_h) to shift the transfer function to the left (Fig. 8A, inset). As V_h was decreased, the number of striatal ensembles activated on each trial increased (Fig. 8A, line, right y-axis), and the proportion of trials on which the shape chosen matched the direction chosen decreased (Fig. 8A, bars, left y-axis). The minimum number of activated striatal ensembles at the end of a trial would be expected to be three (Fig. 8B, $V_h = 16$, shape and direction matched, activated ensembles circled): one each in cognitive and motor and, at the intersection of the two, one in association striatum. As V_h was decreased, whole columns and rows in association striatum became activated, leading to cross talk between channels when transferring the information from one loop to another (Fig. 8C, $V_h = 14$, shape and direction did not match).

Fig. 6. Evolution of normalized cognitive corticostriatal synaptic weights for each of the four cues. Weights at each trial are averaged over 250 runs. Shaded bars represent standard deviation. The average weight for the $P(R) = 1$ cue reaches 0.93 (SD 0.018) at the 60th trial. The average weight for the $P(R) = 0$ cue declines gradually, but has only decreased to 0.44 (SD 0.045) by the final trial. The average weight for the $P(R) = 0.66$ cue is still increasing at the end of the simulation, and therefore the difference from the weight of the best cue is still decreasing. The error bars for the probabilistic cues are larger than for the deterministic cues. Inset: evolution of weights from one run. The changes are more steplike, as not every cue is seen or chosen in every trial. In this particular run, the weights of the $P(R) = 0.33$ and $P(R) = 0$ cues were virtually identical over most of the simulation, but the wrong cue was only chosen once in 20 presentations of this combination.



Robustness to noise. The presence of synaptic noise is necessary to induce symmetry breaking, thus allowing action selection, before learning, without introducing an artificial bias between channels. However, it was possible that this necessary level of noise before learning would interfere with the learned cue-response association and reduce the system's performance after learning. To investigate the robustness of the model to noise, simulations were performed with increasing levels of synaptic noise. The noise was inserted in the model as an additional synaptic input current, simulating the effect of variable packet size and variable rates of synaptic transmission failure. The noise value was drawn independently at each time step from a Gaussian distribution with zero mean and a standard deviation of a proportion of the mean total synaptic input to the neurons. Simulations were performed with the same noise level inserted into all structures. At each level of noise, 50 runs of 120 trials were performed.

Figure 9, top, shows the proportion of trials where the optimum target was chosen. Final performance decreases with increasing noise levels, falling to 0.7 in the last 30 trials with 30% noise. The performance in the final 30 trials is better than in the first 30 for all levels below 100%, showing that there is learning, even with high amounts of noise. The proportion of trials on which the cue shape chosen was consistent with the direction is shown in Fig. 9, bottom. As with the optimum performance, this decreased with increasing noise, falling to 0.73 with 40% noise, with little difference between the first and last 30 trials for all noise levels.

Overall, even for high levels of noise, the change in corticostriatal synaptic weights was sufficient to guide the correct cue-response behavior after learning, and reasonable amounts of noise only marginally affected the performance of the system at the end of learning.

Requirement for association cortex inputs. The open-loop input to associative striatum is a high-level visual representation of a conflation of cue shape and position arising from association cortex. Simulations were performed to determine if this input was necessary in the model. To this end, the weight of inputs from association cortex to associative striatum was set to zero. To provide sufficient input to activate the striatal projection neurons, the weights of inputs from cognitive and motor cortex to associative striatum were increased from 0.2 to

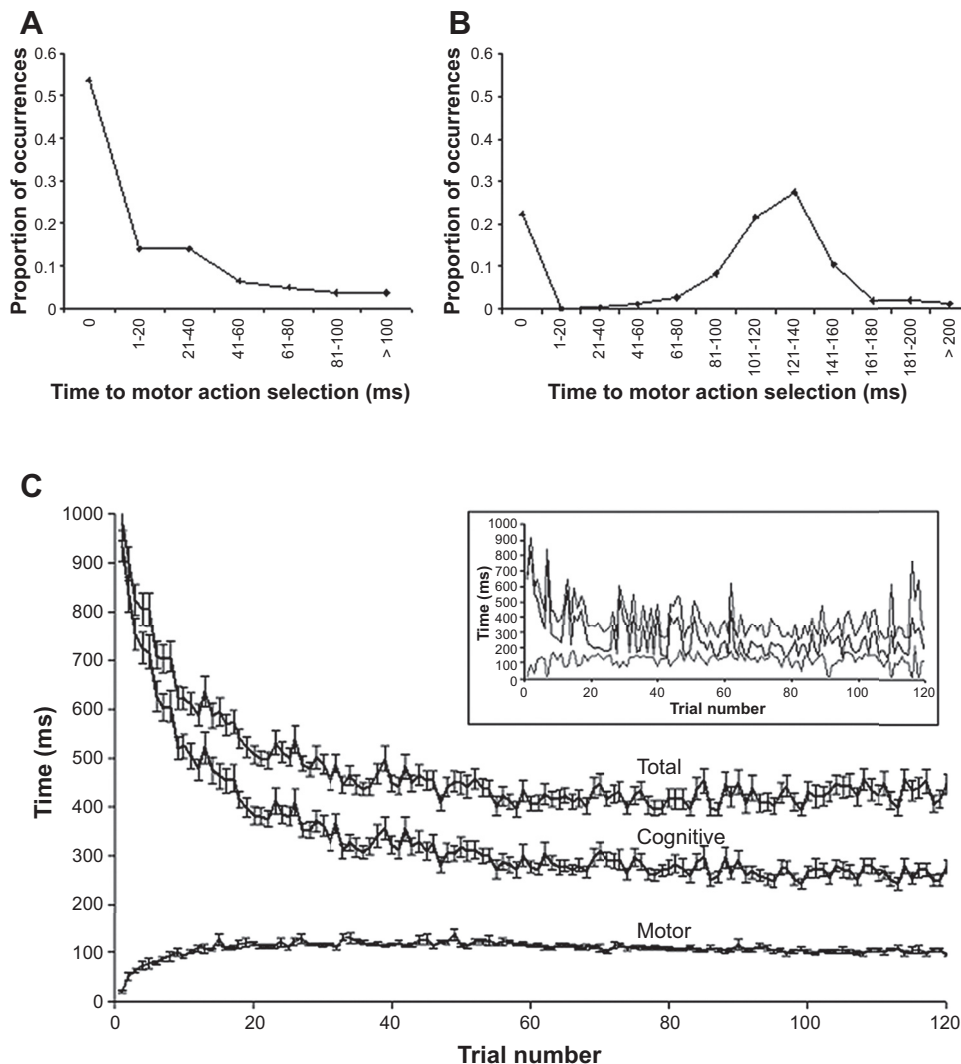


Fig. 7. The average time taken for action selection over 120 trials decreases with learning. Data was averaged over 250 runs. Average time taken to motor action selection on the first trial (A) and the 120th trial (B) is shown. In the first trial, the motor action selection was made before the cognitive action selection approximately one-half of the time, giving a time to motor action selection of zero. In the last trial, the cognitive action selection tended to occur 60–160 ms before the motor action selection. Some trials continued to have a motor action selection time of zero due to having only small differences between synaptic weights. C: the total time taken decreases with learning, as does the time taken for the cognitive decision. The time taken for the motor decision increases to an asymptote after 20 trials. Bars are standard error. *Inset*: decision durations for a single run showing the greatly increased variation compared with the average with periods of slower decision making possibly demonstrating exploration.

0.3. The model was still able to select a direction with a 98.4% success rate. On comparison with the model having association cortex inputs, there was no reliable difference in success rate (trials in which a motor action was performed), but the proportion of optimum trials decreased significantly from 0.91 (SD 0.078) to 0.50 (SD 0.072) ($P < 0.01$ Wilcoxon rank sum test), and the proportion of rewarded trials decreased from 0.74 (SD 0.05) to 0.49 (SD 0.078) ($P < 0.01$ Wilcoxon rank sum test) (Fig. 10). There was no significant change in the time taken for the selection of a direction. The number of striatal units activated at the end of action selection increased from 4.09 (SD 0.12) to 7.74 (SD 0.70). When the weight of the corticostriatal connections to associative striatum was set back to 0.2, action selection did not occur (data not shown).

Striatal and pallidal neurons encode multiple parameters. This double-arm bandit task was originally developed for an experimental approach in primates (Pasquereau et al. 2007). Using a multiparametric analysis, it was shown that striatal and pallidal neurons covary with various task parameters during the decision, such as the value of the chosen shape, the nonchosen shape, both, and/or the direction of the movement (Garenne et al. 2011). This demonstrated that both structures encoded the value of the action by a reshaping of the neuronal tuning curves

by the choice value (Pasquereau et al. 2007), and that the modulation of the neuronal activity in the GPi predicts faithfully the animal's choice (Garenne et al. 2011). We therefore compared neuronal ensembles in the striatum and GPi, both in the experimental data set and in data simulated from our model using a three-way ANOVA (Selected Shape \times Unselected Shape \times Direction, $P < 0.05$). We found neurons encoding the value of the selected shape, the value of the unselected shape, the direction of movement, and the action value (selected shape \times direction of movement) in both striatum and GPi in the model data (Fig. 11). The distribution is slightly different in the model from the recorded data, but it is difficult to infer anything from this difference because of various biases (sampling bias during recording, etc.).

DISCUSSION

It has previously been shown that the center-surround architecture of Mink (1996) provides a credible model for action selection (Gurney et al. 2001; Leblois et al. 2006; Redgrave et al. 1999). In the present study, the model of Leblois (2006) has been extended in three main directions based on the anatomy and physiology of the basal ganglia. Each of these extensions has produced emergent network properties that are in agree-

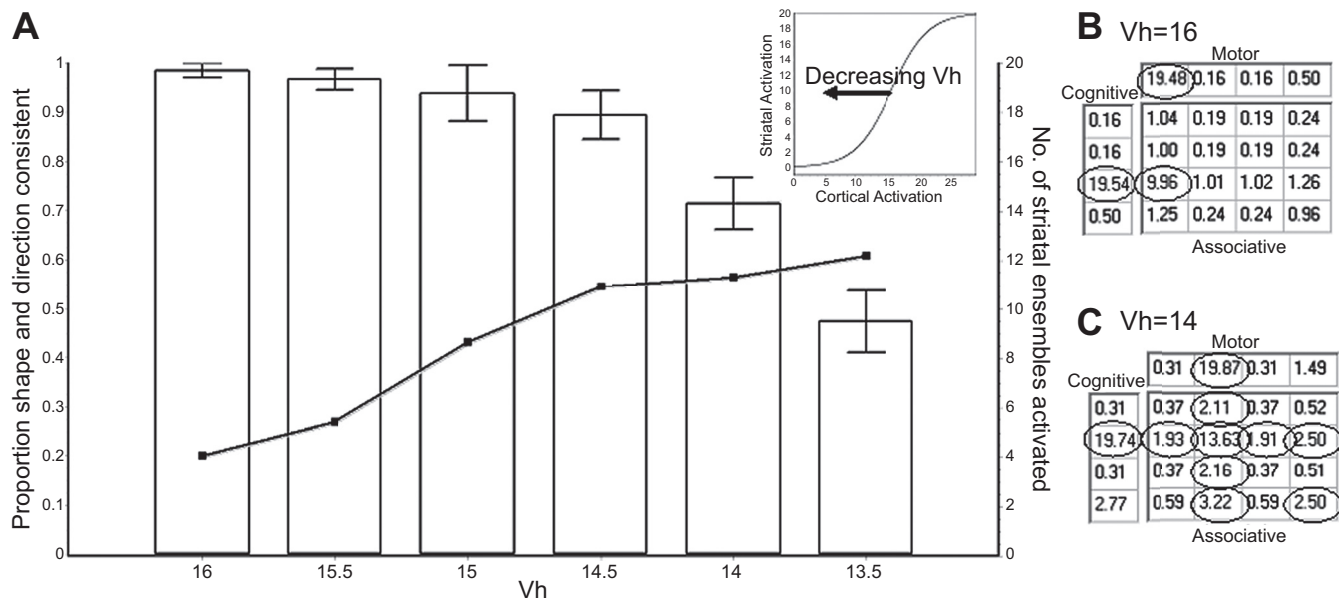


Fig. 8. The effect of shifting the striatal transfer function to the left on the proportion of trials in which the shape chosen matched the direction chosen. *A*, bars: the proportion of the 120 trials, averaged over 50 runs, where the shape chosen matched the direction chosen (left axis), error bars are standard deviation. Line: average number of striatal ensembles activated on each trial as a function of the striatal transfer function half-activation parameter, V_h (right axis). The lower the number of striatal ensembles activated, the better the performance of the model in terms of intraloop information transfer. *Inset*: striatal transfer function with $V_h = 16$. Decreasing V_h shifted the transfer function curve to the left so that striatal ensembles could be activated by lower levels of cortical input. *B*: representative final striatal activations for a trial where $V_h = 16$, before learning. Three striatal ensembles are activated (circled): one cognitive, one motor, and one associational ensemble at the intersection of the two. *C*: representative final striatal activations for a trial where $V_h = 14$, before learning. In this trial, the shape chosen did not match the direction. The whole associational striatal row receiving collaterals from cognitive cortex is activated, as well as the associational column receiving collaterals from motor cortex. Interloop information transfer has failed due to striatal overactivation.

ment with known experimental findings, without losing the four dynamic regimes seen in the model of Leblois et al. (2006). First is the use of synaptic noise to cause the symmetry breaking that leads to action selection during the exploration phase, before the values of the cues are learned. This is in marked contrast to previous models where action selection has been initiated by setting one input higher than the other. Second, a second parallel loop was added to model two different levels of action selection. This incorporates the suspected anatomical cross-connections between CBG loops and gives rise to the property that the action selection at one level can influence the selection at the other level. Additionally, for this transfer of information between loops to be accurate, most striatal units have to remain silent, an emerging property that fits with known striatal electrophysiology. Third, action selection can be learned in a realistic manner using a simulated dopamine error prediction signal. The learning occurs at a rate comparable to that seen in nonhuman primates performing the same task and results in activation of GPi ensembles to various task parameters in proportions similar to those found in nonhuman primates (Garenne et al. 2011; Pasquereau et al. 2007). With learning, units representing different task parameters are found in all areas of model GPi, an electrophysiological finding that has questioned the existence of segregated CBG loops, but is here explained by the interloop information transfer.

Comparison of action selection mechanisms. To resolve the competition and select only one of the possible actions, it is necessary to implement a form of “winner takes all” network. Many previous computational models of action selection have relied on a striatal competition network based around a mutual lateral inhibition mechanism (Alexander and Wickens 1993; Bar-Gad and Bergman 2001; Groves 1983; Koter and Wickens

1998; Suri and Schultz 1999; Woodward et al. 1995) or an equivalent algorithm that implies the lateral inhibition (Frank 2005; Frank et al. 2001; O’Reilly and Frank 2005). This was based anatomically on the extensive recurrent dendritic field of the inhibitory projection neurons of the striatum, medium spiny neurons (MSNs) that, potentially, innervate thousands of other local MSNs (Oorschott 1996) and could, therefore, implement a lateral inhibition network where the activity of the dominant neuron would suppress the activity of all other local neurons. When demonstrated experimentally, recurrent inhibition has been found to be very weak compared with feed-forward inhibition (Jaeger et al. 1994; Koos et al. 2004; Tunstall et al. 2002), with no studies reporting any instances of mutual inhibition between two MSNs and synapses on tertiary dendrites that are electrically distant from the soma. Also, MSNs are mostly silent in anesthetized rats (Wilson and Groves 1981), display very sparse activity in freely moving rats in vivo (Kiyatkin and Rebec 1996), and require a barrage of coordinated excitatory input to induce firing (Wilson 1995). These findings combined throw doubt on the efficacy of a lateral inhibition based “winner takes all” mechanism in the striatum.

An alternative role for lateral inhibition in creating synchronized striatal ensembles has been proposed (Carrillo-Reid et al. 2008). The resting membrane potential of the MSN is hyperpolarized, a so-called down state (O’Donnell and Grace 1995; Wilson and Kawaguchi 1996). As the reversal potential of inhibitory inputs is approximately -65 mV (Kita 1996), and therefore greater than the resting membrane potential, GABAergic inputs in the down state provide shunting inhibition, lifting the membrane potential. Inhibitory inputs to MSNs have been shown to prolong striatal depolarization plateaus (Florès-Barra et al. 2009). Cortical stimulation of striatal slice prepara-

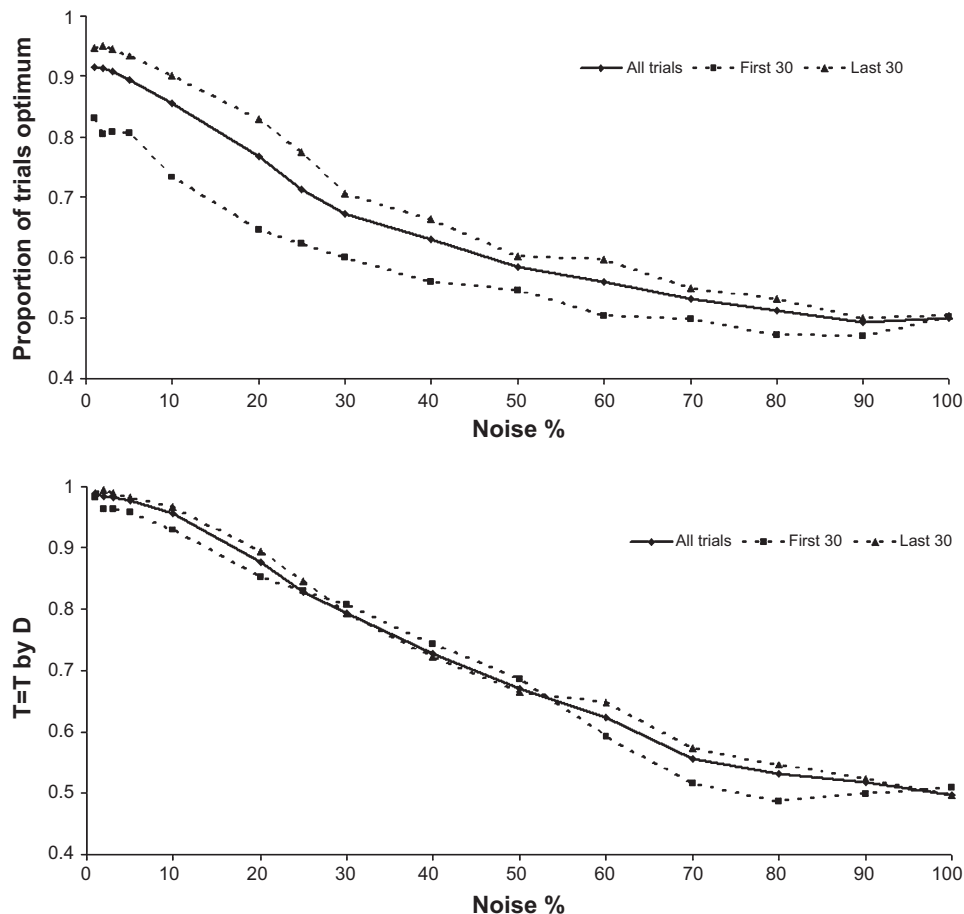


Fig. 9. Robustness of learning and interloop information transfer to synaptic noise. Gaussian noise with a zero mean was applied to synaptic inputs to all structures. The standard deviation of the noise (measured as a proportion of the total synaptic input) was varied on all synaptic inputs to assess model robustness. 50 runs of 120 trials were performed for each level of noise. *Top*: with increasing levels of synaptic noise, the proportion of trials in which the optimum target was chosen decreased, but there was always learning between the first 30 (*lower dashed line*) and last 30 trials (*upper dashed line*). *Bottom*: with increasing levels of synaptic noise, the proportion of trials in which the cue shape and direction were consistent ($T = T$ by D), averaged over all trials, decreased, but did not change with learning.

tions results in synchronized activation of groups of 20–30 MSNs (Carrillo-Reid et al. 2008). Application of a GABA_A antagonist desynchronized these ensembles. These findings suggest that the role of lateral inhibition between MSNs is to synchronously activate an ensemble of neurons. Such a proposal is the opposite of a lateral inhibitory “winner takes all” network and could be described as a lateral inhibitory striatal ensemble. In addition Carrillo-Reid et al. (2008) noted that there was a small degree of overlap in the neurons activated in

different ensembles. This fits in with the proposed architecture of the associative stratum where the convergence of cognitive and motor cortical inputs would activate individual neurons in more than one ensemble. To fit with the architecture used in the current model, it would also be necessary to show that the output of a striatal ensemble reconverged at the GPi level. While it has been shown that a retrograde tracer injected into GPi labels several distinct areas in striatum (Flaherty and Graybiel 1993), to verify the model architecture would require that the anterograde activation from cortex be shown to overlap with the retrograde labeling. The current model demonstrates a viable mechanism for action selection. If lateral inhibition were present in the striatum, this would be complementary to the network mechanism presented here and would serve to enhance the efficiency of basal ganglia action selection.

Role of the hyperdirect pathway. In this model, the hyperdirect pathway provides a divergent negative feedback to all the channels in its own loop. This acts to suppress all nonselected channels. Other functions have also been proposed for this pathway. In the original center surround architecture of Mink (1996), the hyperdirect pathway acted to suppress all channels at the start of an action selection process because of its shorter conduction times than the direct and indirect pathways. This could be interpreted as a sort of clear function, but has more recently also been used as a switch function (Isoda and Hikosaka 2008). Such a function would be compatible with the function of the hyperdirect pathway modeled here and would provide an extension for modeling sequential decisions.

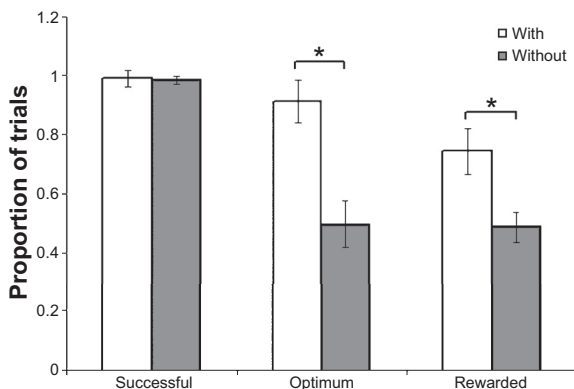


Fig. 10. Comparison of performance with and without association cortex inputs. With the weight of the association cortex input to associative striatum set to zero, there was no reliably significant decrease in the proportion of the 120 trials, averaged over 50 runs, where the model was able to make a decision (successful). The proportion of trials where the optimum direction was chosen and the proportion of trials rewarded decreased significantly without association cortex input (* $P < 0.01$ Wilcoxon rank test).

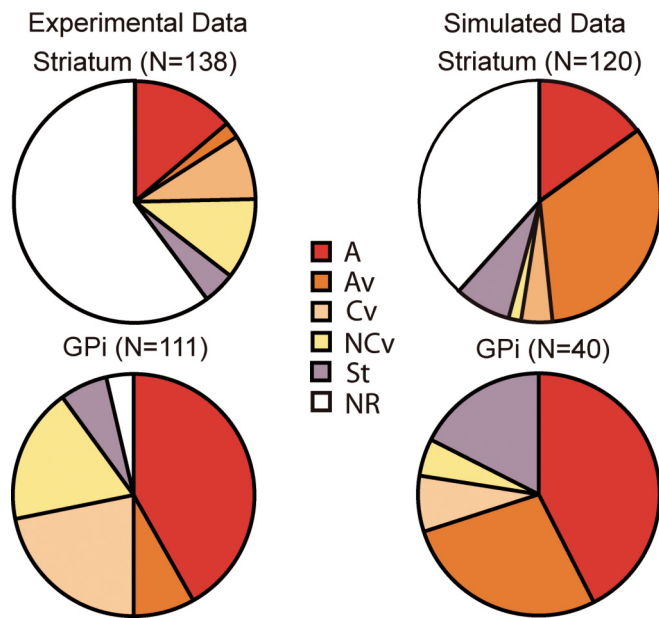


Fig. 11. Comparison of task parameters in experimental and model neurons in striatum and GPi. Experimental data from Pasquereau et al. (2007) are shown on the *left*. Both striatum and GPi code for many parameters at the start of movement. Simulated data (*right*) show that, in striatum and GPi, there are more neurons coding for the action value and less not reacting to any parameter than in the experimental data. A, action; Av, action value; Cv, chosen cue value; NCv, nonchosen cue value; St, state value; NR, nonreacting.

Role of the indirect pathway. An indirect pathway has not been included in this modeling study for various reasons. In the first instance, the aim of the study was to use the minimal circuitry necessary to demonstrate two-level decision making. Roles proposed for the indirect pathway include capacity scaling (Gurney et al. 2001) and as a NoGo pathway (Frank 2005; Frank et al. 2001). Neither of these roles was relevant to the task under consideration, but further discussion of these points can be found in Leblois et al. (2006). Future studies are planned to include a role for this pathway in controlling duration of action selection.

Network learning. Before learning, there is no reason to choose one cue over any other, which is reflected in the model by starting corticostriatal weights for all cues being the same (with some initial variation). When the relative gains of the direct and hyperdirect pathways placed the model in the symmetry breaking area of phase space, action selection was induced by the presence in the model of reasonable levels of synaptic noise, such as those found experimentally in the GPi (Boraud et al. 2000; Brotchie et al. 1991). Before learning, this provides a mechanism to perform a random action selection that can start the exploration of the space of action values. Another mechanism that has been proposed for this exploration phase is chaotic activity within the globus pallidus externa-STN loop (Chakravarthy et al. 2010; Kalva et al. 2012). This mechanism is not incompatible with the synaptic noise used here and would provide an interesting extension to this model, allowing the study of control of the exploration phase.

Learning within the model was implemented only at the corticostriatal synapses and was sufficient to produce rapid learning with an exploratory and an exploitative phase. The evolution of corticostriatal weights for the four cues shows a divergence within the first 30 trials (Fig. 6), which is sufficient

to increase the performance of the model from chance to a probability of 0.9 in choosing the optimum cue (Fig. 5). This implies that, at this point, it is no longer synaptic noise driving the action selection, but the learned values of the cues reflected in their relative corticostriatal synaptic weights. This change in synaptic weights provides the bias between the two channels such that identical cortical input signals are differentiated. When the bias provided by the learned synaptic weights takes over action selection, the noise that was necessary for action selection at the start of learning does not impair learned performance. Indeed, the model was very resistant to noise, and optimal cue-response associations were still performed in more than 70% of the trials for noise levels as high as 30% of the mean external synaptic input in all structures (Fig. 9A). Such a high level of robustness to noise is a somewhat surprising emergent property of the model architecture. The basal ganglia have also been shown to be involved in reversal learning (Cools et al. 2001; Lawrence et al. 1999). The minimal decreases in the corticostriatal weights for the worst cues (Fig. 6) suggest that this model architecture would be able to rapidly reverse choice behavior when reward contingencies are changed.

To concentrate on the function of the actor in decision making, the critic has been modeled at a very basic level to track the value of cues. We are currently developing a biophysically based model of critic learning that we hope to ally with our model of the actor in future studies to extend the model functionality to a full actor-critic representation.

Two-level action selection. The main extension made for this version of the action selection model was the addition of a second, parallel, partially segregated CBG loop. This was based on both theoretical considerations and electrophysiological data. A decision made at a higher cognitive level, such as deciding to seek food rather than drink, must influence lower level decisions to be acted upon. This hierarchy of decision making was visible in the data from Pasquereau et al. (2007) because the experimental design included two decision points, separated in time: first when the cue shapes are shown, and then when the signal to make a movement was given. This temporal separation should not be necessary for multilevel decision making but exposed the two-stage neuronal reaction. Given that action selection is a property of a segregated CBG loop, for one level of decision making to influence another, there must be information transfer between the loops involved in different levels. This property of the model provides an opportunity to reconcile the debate between segregated and overlapping direct pathway corticostriatal loops by suggesting an architecture where each segregated loop processes decision making at its own level and makes available the results of that decision to other levels via cross talk between the loops. We have here implemented this information transfer as a divergence of inputs from cortex to striatum followed by an orthogonal reconvergence from striatum to GPi. While this seems a reasonable interpretation of the known anatomy (see MATERIALS AND METHODS, *Model architecture*, Figs. 1 and 3), it is not crucial to the model function, and other schemes of information transfer could be proposed. The model design allows bidirectional information transfer between loops, a consequence of which was that, in early trials, a direction could be selected before a shape leading to a motor bias of cue selection. In this situation, the correct shape was generally well on the

way to being selected (Fig. 4, *inset*) and was thus correctly reinforced during the learning phase. Whether such a mechanism is present in the animal basal ganglia is not clear and would require the design of an experiment that could be run with learning of cue values at either of two levels. Anatomical evidence from the dopaminergic critic system suggests that there is a spiral of influence running from ventromedial to dorsolateral basal ganglia regions (Haber et al. 2000). However, because neurons that encode motor parameters are found throughout the GPi (Garenne et al. 2011), this directionality of influence is unlikely to be present in the actor structures. We would predict that an experiment where the value was based on the motor action, not the cognitive action selection, would still lead to activation of neurons in GPi to cognitive aspects of the cue.

With learning, the time for action selection decreased (Fig. 7). The time from cue onset to the cognitive decision was always greater than the subsequent time from cognitive decision to the motor decision. This is because the transfer of information from the cognitive to the motor loop started as soon as the two channels in the cognitive loop started to diverge and did not have to wait until the cognitive action selection had been completed (Fig. 4). This means that the interloop information transfer allows parallel processing in multiple loops rather than sequential decision making from one loop at a time, a property that would decrease the time taken for multilevel decision making.

Interloop information transfer. Using this architecture, interloop information transfer was effective, with the direction matching to the shape in over 99% of trials, thus enabling accurate two-stage action selection. This did not significantly change between the early and late periods of the learning protocol, showing that this is an intrinsic property of the connectivity of the model and not related to the learning. As the striatal transfer function curve was shifted to the left by decreasing the half-activation parameter, V_h , the proportion of trials in which the shape matched the direction decreased drastically alongside a parallel increase in the number of striatal units activated (Fig. 8). This suggests that, for accurate interlevel information transfer, it is necessary to activate only those association striatal units that have convergence from both sensory levels of one cue (shape and direction). As the number of activated striatal units increases, association striatal units with convergence of one sensory level from each of two different cues (i.e., the shape from one cue and the direction from another) increases, leading to possible selection of the wrong direction, even when the more valued shape is chosen. The advantages accruing from the ability to accurately perform multilevel selection suggest that such a system would emerge from evolution in a neuro-Darwinian fashion. The known properties of the striatal projection neurons, including the hyperpolarized resting state due to an inwardly rectifying potassium current (Jiang and North 1991; Nisenbaum and Wilson 1995) and the requirement for a concerted excitatory barrage to depolarize the neurons to the firing threshold (Wilson 1995), provide a network that has the required properties for accurate interloop information transfer.

The distribution of neurons that encode each parameter of the action selection in striatum and GPi are slightly different to those found in monkeys and show that motor parameters can be represented in cognitive areas and vice versa. The most striking

difference is an oversized population which encodes Action Value at the striatal level and to a lesser extent in the GPi in the model. This may be accounted for because the monkeys were overtrained over a considerable period to prelearn the shape values before the behavioral measurements and electrophysiological recordings were made. This may also have led to some transfer to cortical learning that is beyond the scope of the present model (Pasupathy and Miller 2005; Turner and Desmurget 2010). Also, we have only modeled the neurons involved in the task under consideration, whereas neurons recorded in the monkey, especially in the striatum, may well not be involved in performance of the task. However, the critical point here is that the heterogeneity of the neuronal correlation with task parameters emerges from the dynamic properties of the network. Neurons belonging to the same subpopulations and involved in the same networks can covary with different parameters according to the randomness of their connectivity properties. This also provides an explanation for why anatomical and electrophysiological studies provide a conflicting picture of the separation of loops in the GPi. For example, neurons belonging to the motor loop (i.e., projecting back to motor cortical area through the thalamus) can covary with cognitive parameters such as cue shape value.

Within the basal ganglia, there are more than two parallel loops. The actual number of separate loops is debated, but, for instance, motor, oculomotor, prefrontal, and limbic have been described (Alexander and Crutcher 1990). This would allow decision making at multiple levels. Clearly the architecture of this model could be extended to incorporate more parallel loops. Whether such a model would require communication only between adjacent loops or between all loops simultaneously is not clear. From a theoretical point of view, it would not seem advantageous to communicate across multiple levels because a high-level need, such as thirst, would not be able to sensibly inform a decision on movement without an intervening decision level based on the value of the current environmental cues to satisfy the need. This would suggest that it is more likely that parallel loops communicate mainly with adjacent loops.

Learning of action selection outside the basal ganglia. This model considers only decision making implemented by CBG loops, with learning at the level of the striatum. There have been many studies that also show decision-making processes in parietal cortex (Bollimunta et al. 2012; Platt and Glimcher 1999; Shadlen and Newsome 2001), prefrontal cortex (Bechara et al. 1999; Hoshi et al. 1999; Rainer et al. 1998), orbitofrontal cortex (Padoa-Schioppa and Assad 2006; Wallis and Miller 2003), dorsolateral cortex (Wallis and Miller 2003), premotor cortex (Cisek and Kalaska 2005; Hernández et al. 2002; Schall 2001), and superior colliculus (McPeck and Keller 2002; Wurtz and Albano 1980). Most of these areas are connected to CBG loops where the cortical activity observed could be that observed in the cortical ensembles during action selection in this model. However, there is also learning in these areas, and decision making may be occurring in parallel to that of the CBG loops. Pasupathy and Miller (2005) showed that the basal ganglia learning was more rapid than prefrontal cortical and suggested that the basal ganglia trains the cortex. Based on this, learning in the current model was restricted to corticostriatal synapses with the possibility of examining cortical transfer in later versions.

Role of association cortex. When the association cortex was lesioned, the model was unable to perform accurate two-level decision making, choosing the optimum direction significantly less often (Fig. 10). This shows that the model requires a conflation of the different sensory aspects of the cues to correctly pass decision making from one level to another. If there is no visual association between cue shape and direction, the model cannot create that association itself and will therefore randomly choose a direction, no matter what shape is chosen.

It has been shown that subjects suffering from amnesic mild cognitive impairment, a precursor of Alzheimer's disease where the medial temporal lobe is damaged, also have problems with complex decision making (Myers et al. 2003; Nagy et al. 2007), although different from those seen in Parkinson's disease. Based on the findings here, we would predict that these deficits are due to an inability to conflate the sensory dimensions of a task as an input to the basal ganglia.

Conclusion. In ethological situations, animals generally have to perform multiple-level decision making to satisfy goals, e.g., a primary need, such as thirst, has to bias multiple lower cognitive and motor levels of decision making in a coordinated fashion to satisfy the need. The basal ganglia are in a privileged position, receiving cortical input representing all levels of possible choices into feedback loops that are largely separated for the different levels of decision making. In this model, we show how decision making could be processed in each parallel loop and the results at one level passed to the next. The unusual electrophysiological properties of the striatal projection neurons have long been of interest, but the functional significance of the difficulty of making them fire has not been obvious. The findings of this model suggest that this is the precise property that is required to learn accurate multilevel decision making. With this property, multilevel decision making becomes an emergent property of the basal ganglia network.

ACKNOWLEDGMENTS

We thank David Hansel for discussions on modeling techniques, and Benjamin Pasquereau for supplying electrophysiological data from recording experiments in monkeys.

GRANTS

M. Garenne was funded by Centre National de la Recherche Scientifique and Agence Nationale de la Recherche (ANR). The project was funded by ANR (Projets Exploratoires Pluridisciplinaires Grant 09-MNPS-017-01).

DISCLOSURES

No conflicts of interest, financial or otherwise, are declared by the author(s).

AUTHOR CONTRIBUTIONS

Author contributions: M.G., A.L., and T.B. conception and design of research; M.G. performed experiments; M.G. and A.G. analyzed data; M.G. and A.L. interpreted results of experiments; M.G. prepared figures; M.G. drafted manuscript; M.G. and T.B. edited and revised manuscript; T.B. approved final version of manuscript.

REFERENCES

Albin R, Penney J, Young A. The functional anatomy of basal ganglia disorders. *Trends Neurosci* 12: 366–375, 1989.

Alexander G, De Long M, Strick P. Parallel organization of functionally segregated circuits linking basal ganglia and cortex. *Annu Rev Neurosci* 9: 357–381, 1986.

Alexander G, Crutcher M. Functional architecture of basal ganglia circuits: neural substrates of parallel processing. *Trends Neurosci* 13: 266–271, 1990.

Alexander G, Crutcher M, De Long M. Basal ganglia-thalamocortical circuits: parallel substrates for motor, oculomotor, “prefrontal” and “limbic” functions. *Prog Brain Res* 85: 119–146, 1991.

Alexander M, Wickens J. Analysis of striatal dynamics: the existence of two modes of behaviour. *J Theor Biol* 163: 413–438, 1993.

Bar-Gad I, Bergman H. Stepping out of the box: information processing in the neural networks of the basal ganglia. *Curr Opin Neurobiol* 11: 689–695, 2001.

Barto A. Adaptive critics and the basal ganglia. In: *Models of Information Processing in the Basal Ganglia*, edited by Houk JC, Davis JL, Beiser DG. Cambridge, MA: MIT Press, 1995, p. 215–232.

Bechara A, Damasio H, Damasio AR, Lee GP. Different contributions of the human amygdala and ventromedial prefrontal cortex to decision-making. *J Neurosci* 19: 5473–5481, 1999.

Bollimunta A, Totten D, Ditterich J. Neural dynamics of choice: single-trial analysis of decision-related activity in parietal cortex. *J Neurosci* 32: 12684–12701, 2012.

Boraud T, Bezard E, Bioulac B, Gross C. Ratio of inhibited-to-activated pallidal neurons decreases dramatically during passive limb movement in the MPTP-treated. *J Neurophysiol* 83: 1760–1763, 2000.

Brotchie P, Iansel R, Horne MK. Motor function of the monkey globus pallidus. I. Neuronal discharge and parameters of movement. *Brain* 114: 1667–1683, 1991.

Brown J, Bullock D, Grossberg S. How the basal ganglia use parallel excitatory and inhibitory learning pathways to selectively respond to unexpected reward. *J Neurosci* 19: 10502–10511, 1999.

Brown LL, Smith DM, Goldbloom LM. Organizing principles of cortical integration in the rat neostriatum: corticostriate map of the body surface is an ordered lattice of curved laminae and radial points. *J Comp Neurol* 392: 468–488, 1998.

Carrillo-Reid L, Tecuapetla F, Tapia D, Hernandez-Cruz A, Galarraga E, Drucker-Colin R, Vargas J. Encoding network states by striatal cell assemblies. *J Neurophysiol* 99: 1435–1450, 2008.

Chakravarthy VS, Joseph D, Bapi RS. What do the basal ganglia do? A modeling perspective. *Biol Cybern* 103: 237–253, 2010.

Chevalier JM, Deniau G. Disinhibition as basic process in the expression in striatal functions. *Trends Neurosci* 13: 277–280, 1990.

Cisek P, Kalaska J. Neural correlates of reaching decisions in dorsal premotor cortex: specification of multiple direction choices and final. *Neuron* 45: 801–814, 2005.

Cools R, Barker RA, Sahakian TW, Robbins BJ. Enhanced or impaired cognitive function in Parkinson's disease as a function of dopaminergic medication and task demands. *Cereb Cortex* 11: 1136–1143, 2001.

Cowan RH, Wilson CJ. Spontaneous firing patterns and axonal projections of single corticostriatal neurons in the rat medial agranular cortex. *J Neurophysiol* 71: 17–32, 1994.

Flaherty AW, Graybiel AM. Corticostriatal transformations in the primate somatosensory system. Projections from physiologically mapped body-part representations. *J Neurophysiol* 66: 1249–1263, 1991.

Flaherty AW, Graybiel AM. Output architecture of the primate putamen. *J Neurosci* 13: 3222–3237, 1993.

Flaherty AW, Graybiel AM. Input-output organization of the sensorimotor striatum in the squirrel monkey. *J Neurosci* 14: 599–610, 1994.

Flores-Barrera E, Vargas J, Galarraga E, Laville J, Plata V, Tapia D. Inhibitory contribution to suprathreshold corticostriatal responses: an experimental and modeling study. *Cell Mol Biol* 29: 719–731, 2009.

Frank M, Loughry B, O'Reilly R. Interactions between frontal cortex and basal ganglia in working memory: a computational model. *Cogn Affect Behav Neurosci* 1: 137–160, 2001.

Frank M. Dynamic dopamine modulation in the basal ganglia: a neurocomputational account of cognitive deficits in medicated and nonmedicated Parkinsonism. *J Cogn Neurosci* 17: 51–72, 2005.

Garenne A, Pasquereau B, Guthrie M, Bioulac B, Boraud T. Basal ganglia preferentially encode context dependent choice in a two-armed bandit task. *Front Syst Neurosci* 5: 23, 2011.

Graybiel A, Aosaki T, Flaherty A, Kimura M. The basal ganglia and adaptive motor control. *Science* 265: 1826–1831, 1994.

- Groves PM.** A theory of the functional organization of the neostriatum and the neostriatal control of voluntary movement. *Brain Res* 286: 109–132, 1983.
- Gurney K, Prescott T, Redgrave P.** A computational model of action selection in the basal ganglia. I. A new functional anatomy. *Biol Cybern* 84: 401–410, 2001.
- Haber S, Fudge J, McFarland N.** Striatonigrostriatal pathways in primates form an ascending spiral from the shell to the dorsolateral striatum. *J Neurosci* 20: 2369–2382, 2000.
- Hazrati LN, Parent A.** Convergence of subthalamic and striatal efferents at pallidal level in primates: an anterograde double-labeling study with biocytin and PHA-L. *Brain Res* 569: 336–340, 1992a.
- Hazrati LN, Parent A.** Differential patterns of arborization of striatal and subthalamic fibers in the two pallidal segments in primates. *Brain Res* 598: 311–315, 1992b.
- Hazrati LN, Parent A.** The striato-pallidal projection displays a high degree of anatomical specificity in the primate. *Brain Res* 592: 213–227, 1992c.
- Hernández A, Zainos A, Romo R.** Temporal evolution of a decision-making process in medial premotor cortex. *Neuron* 33: 959–972, 2002.
- Hopfield JJ.** Neurons with graded response have collective computational properties like those of two-state neurons. *Proc Natl Acad Sci U S A* 81: 3088–3092, 1984.
- Hoshi E, Keisetsu S, Tanji J.** Neuronal activity in the primate prefrontal cortex in the process of motor selection based on two behavioral rules. *J Neurophysiol* 83: 2355–2373, 1999.
- Itti L, Koch C.** Computational modelling of visual attentions. *Nat Rev Neurosci* 2: 194–203, 2001.
- Jaeger D, Kita H, Wilson C.** Surround inhibition among projection neurons is weak or nonexistent in the rat neostriatum. *J Neurophysiol* 72: 2555–2558, 1994.
- Jiang Z, North R.** Membrane properties and synaptic responses of rat striatal neurones in vitro. *J Physiol* 443: 533–553, 1991.
- Kalva SK, Rengaswamy M, Chakravarthy VS, Gupte N.** On the neural substrates for exploratory dynamics in basal ganglia: a model. *Neural Netw* 32: 65–73, 2012.
- Kerr JN, Wickens JR.** Dopamine D-1/D-5 receptor activation is required for long-term potentiation in the rat neostriatum in vitro. *J Neurophysiol* 85: 117–124, 2001.
- Kincaid AE, Penney JB, Young AB, Newman SW.** The globus pallidus receives a projection from the parafascicular nucleus in rat. *Brain Res* 553: 18–26, 1991.
- Kincaid A, Zheng T, Wilson C.** Connectivity and convergence of single corticostriatal axons. *J Neurosci* 18: 4722–4731, 1998.
- Kita H.** Glutamatergic and GABAergic postsynaptic responses of striatal spiny neurons to intrastriatal and cortical stimulation recorded in slice preparations. *Neuroscience* 70: 925–940, 1996.
- Kiyatkin EA, Rebec GV.** Dopaminergic modulation of glutamate-induced excitations of neurons in the neostriatum and nucleus accumbens of awake, unrestrained rats. *J Neurophysiol* 75: 142–153, 1996.
- Koos T, Tepper J, Wilson C.** Comparison of IPSCs evoked by spiny and fast-spiking neurons in the neostriatum. *J Neurosci* 24: 7916–7922, 2004.
- Kotter R, Wickens JR.** Striatal mechanisms in Parkinson's disease: new insights from computer modeling. *Artif Intell Med* 13: 37–55, 1998.
- Lawrence AD, Sahakian BJ, Rogers RD, Hodges JR, Robbins TW.** Discrimination, reversal, and shift learning in Huntington's disease: mechanisms of impaired response selection. *Neuropsychologia* 37: 1359–1374, 1999.
- Leblois A, Boraud T, Meissner W, Bergmann H, Hansel D.** Competition between feedback loops underlies normal and pathological dynamics in the basal ganglia. *J Neurosci* 26: 3567–3583, 2006.
- McPeck RM, Keller EL.** Saccade target selection in the superior colliculus during a visual search task. *J Neurophysiol* 88: 2019–2034, 2002.
- Mink J.** The basal ganglia: focused selection and inhibition of competing motor programs. *Prog Neurobiol* 50: 381–425, 1996.
- Myers C, Shohamy D, Gluck M, Grossman A, Kluger S, Ferris S, Golomb J, Schirman G, Schwartz R.** Dissociating hippocampal versus basal ganglia contributions to learning and transfer. *J Cogn Neurosci* 15: 185–193, 2003.
- Nagy H, Keri S, Myers C, Benedek G, Shohamy D, Gluck M.** Cognitive sequence learning in Parkinson's disease and amnesic mild cognitive impairment: dissociation between sequential and non-sequential learning of associations. *Neuropsychologia* 45: 1386, 2007.
- Nambu A, Takada M, Inase M, Tokuno H.** Dual somatotopical representations in the primate subthalamic nucleus: evidence for ordered but reversed body-map transformations from the primary motor cortex and the supplementary motor area. *J Neurosci* 16: 2671–2683, 1996.
- Nambu A, Tokuno H, Hamada I, Kita H, Imanishi M, Akazawa T, Ikeuchi Y, Hasegawa N.** Excitatory cortical inputs to pallidal neurons via the subthalamic nucleus in the monkey. *J Neurophysiol* 84: 289–300, 2000.
- Nisenbaum E, Wilson C.** Potassium currents responsible for inward and outward rectification in rat neostriatal spiny projection neurons. *J Neurosci* 15: 4449–4463, 1995.
- O'Donnell P, Grace AA.** Synaptic interactions among excitatory afferents to nucleus accumbens neurons: hippocampal gating of prefrontal cortical input. *J Neurosci* 15: 3622–3639, 1995.
- Oorschot DE.** Total number of neurones in the neostriatal, pallidal, subthalamic, and substantia nigral nuclei of the rat basal ganglia: a stereological study using the cavalieri and optical disector methods. *J Comp Neurol* 366: 580–599, 1996.
- O'Reilly R, Frank M.** Making working memory work: a computational model of learning in the prefrontal cortex and basal ganglia. *Neural Comput* 18: 283–328, 2005.
- Padoa-Schioppa C, Assad JA.** Neurons in the orbitofrontal cortex encode economic value. *Nature* 441: 223–226, 2006.
- Parent A, Hazrati LN.** Functional anatomy of the basal ganglia. I. The cortico-basal ganglia-thalamo-cortical loop. *Brain Res Brain Res Rev* 20: 91, 1995.
- Parent A, Sato F, Wu Y, Gauthier J, Levesque M, Parent M.** Organization of the basal ganglia: the importance of axonal collateralization. *Trends Neurosci* 23 (Suppl 10): S20–S27, 2000.
- Parthasarathy HB, Schall JD, Graybiel AM.** Distributed but convergent ordering of corticostriatal projections: analysis of the frontal eye field and the supplementary eye field in the macaque monkey. *J Neurosci* 12: 4468–4488, 1992.
- Pasquereau B, Nadjar A, Arkadir D, Bezdard E, Goillandeau M, Bioulac B, Gross C, Boraud T.** Shaping of motor responses by incentive values through the basal ganglia. *J Neurosci* 27: 1176–1183, 2007.
- Pasupathy A, Miller E.** Different time courses of learning-related activity in the prefrontal cortex and striatum. *Nature* 433: 873–876, 2005.
- Pawlak V, Kerr J.** Dopamine receptor activation is required for corticostriatal spike-timing dependent plasticity. *J Neurosci* 28: 2435–2446, 2008.
- Percheron G, Yehrik J, Francois C.** A Golgi analysis of the primate globus pallidus. III. Spatial organization of the striato-pallidal complex. *J Comp Neurol* 227: 214–227, 1984.
- Platt M, Glimcher P.** Neural correlates of decision variables in parietal cortex. *Nature* 400: 233–238, 1999.
- Rainer G, Asaad W, Miller E.** Selective representation of relevant information by neurons in the primate prefrontal cortex. *Nature* 393: 577–579, 1998.
- Redgrave P, Prescott TJ, Gurney K.** The basal ganglia: a vertebrate solution to the selection problem? *Neuroscience* 89: 1009–1023, 1999.
- Reynolds J, Hyland B, Wickens J.** A cellular mechanism of reward-related learning. *Exp Neurol* 413: 67–70, 2001.
- Sandstrom MI, Rebec GV.** Characterization of striatal activity in conscious rats: contribution of NMDA and AMPA/kainate receptors to both spontaneous and glutamate-driven firing. *Synapse* 47: 91–100, 2003.
- Schall JD.** Neural basis of deciding, choosing and acting. *Nat Rev Neurosci* 27: 33–42, 2001.
- Shadlen M, Newsome W.** Neural basis of a perceptual decision in the parietal cortex (area LIP) of the rhesus monkey. *J Neurophysiol* 86: 1916–1936, 2001.
- Shriki O, Hansel D, Sompolinsky H.** Rate models for conductance based cortical neuronal networks. *Neural Comput* 15: 1809–1841, 2003.
- Suri R, Schultz W.** A neural network model with dopamine-like reinforcement signal that learns a spatial delayed response task. *Neuroscience* 91: 871–890, 1999.
- Takada M, Tokuno H, Hamada I, Inase M, Ito Y, Imanishi M, Hasegawa N, Akazawa T, Hatanaka N, Nambu A.** Organization of inputs from cingulate motor areas to basal ganglia in macaque monkey. *Eur J Neurosci* 14: 1633–1650, 2001.
- Tunstall M, Oorschot D, Kean A, Wickens J.** Inhibitory interactions between spiny projection neurons in the rat striatum. *J Neurophysiol* 88: 1263–1269, 2002.
- Turner RS, Desmurget M.** Basal ganglia contributions to motor control: a vigorous tutor. *Curr Opin Neurobiol* 20: 704–16, 2010.
- Wallis JD, Miller EK.** Neuronal activity in primate dorsolateral and orbital prefrontal cortex during performance of a reward preference task. *Eur J Neurosci* 18: 2069–2081, 2003.

- Webster KE.** Cortico-striate interrelations in the albino rat. *J Anat* 95: 532–545, 1961.
- Wickens JR, Alexander M.** Analysis of striatal dynamics: the existence of two modes of behaviour. *J Theor Biol* 163: 413–438, 1993.
- Wilson CJ, Groves PM.** Spontaneous firing patterns of identified spiny neurons in the rat neostriatum. *Brain Res* 220: 67–80, 1981.
- Wilson CJ.** Morphology and synaptic connections of crossed corticostriatal neurons in the rat. *J Comp Neurol* 1263: 567–580, 1987.
- Wilson CJ.** The contribution of cortical neurons to the firing pattern of striatal spiny neurons. In: *Models of Information Processing in the Basal Ganglia*, edited by Houk JC, Davis JL, Beiser DG. Cambridge, MA: MIT Press, 1995, p. 141–171.
- Wilson CJ, Kawaguchi Y.** The origins of two-state spontaneous membrane potential fluctuations of neostriatal spiny neurons. *J Neurosci* 16: 2397–2410, 1996.
- Wilson HR, Cowan JD.** Excitatory and inhibitory interactions in localized populations of model neurons. *Biophys J* 12: 1–24, 1972.
- Woodward DJ, Kirilov AB, Myre CD, Sawyer SF.** Neostriatal circuitry as a scalar model: modelling and ensemble neuron recording. In: *Models of Information Processing in the Basal Ganglia*, edited by Houk JC, Davis JL, Beiser DG. Cambridge, MA: MIT Press, 1995, p. 315–336.
- Wurtz RH, Albano JE.** Visual-motor function of the primate superior colliculus. *Annu Rev Neurosci* 3: 189–226, 1980.

